arXiv:0911.5039v1 [cond-mat.stat-mech] 26 Nov 2009

Bose-Einstein condensation of semi-hard bosons in S=1 dimerized organic compound F_2PNNNO

I.G. Bostrem, V.E. Sinitsyn, A.S. Ovchinnikov
Department of Physics, Ural State University, 620083, Ekaterinburg, Russia

Y. Hosokoshi
Department of Physical Science, Osaka Prefecture University, Osaka, Japan

K. Inoue
Department of Chemistry, Hiroshima University, Hiroshima, Japan

(Dated: September 15, 2021)

An analysis of the energy spectrum and the magnetization curve of two-dimensional organic antiferromagnet F_2PNNNO with a spin-one dimerized structure shows that a behavior of the compound in an external magnetic field can be explained within a lattice boson model with an extended Pauli's exclusion principle, i.e. no more than two bosons per a dimer. The unusual magnetization curve observed experimentally in the compound reflects a sequence of phase transitions intrinsic for a lattice boson system with strong on-site and inter-site repulsions due to a tuning of magnon density by the applied magnetic field.

I. INTRODUCTION

A possibility to study the Bose-Einstein condensation (BEC) with low-dimensional magnetic materials predicted theoretically twenty years ago[1] gave rise to intense experimental studies in the field. The analogy between the spins and the bosons becomes evident for antiferromagnets where spins form dimers with a spin-singlet ground state.[2] Originally, main attention was focused on spin-1/2 systems where excitations inside each dimer (triplons) are regarded as bosons with hard-core repulsion, i.e. no more than one boson present on a single dimer. The analogy enables to treat the spin systems as that of interacting bosons whose ground state is determined by the balance between the kinetic energy and the repulsive interactions.[3] If the repulsion dominates the bosons will form a superlattice and a finite energy cost is needed to create an additional particle. This exhibits itself as a jump in chemical potential versus boson number, in the spin language, as a plateau in magnetization curve versus magnetic field at rational fraction of saturated magnetization.

The field induced condensation of magnons has been experimentally observed in coupled quantum ($s = 1/2$) dimer systems based on Cu^{2+} ions such as $TlCuCl_3$ and $BaCuSi_2O_6$[4,5,6] and the compound $Ba_2Cr_2O_8$[7] which are adequately described by the BEC theory.

Recently, magnetic weakly coupled dimer system $Ba_3Mn_2O_8$ with $S = 1$ moments attracted a lot of attention.[8,9] The field behavior of magnetization in the system of antiferromagnetically weakly coupled $S = 1$ dimers can be described as BEC of magnons by mapping the spin-1 system into a gas of semi-hard-core bosons.[10] On an example of simple two-dimensional (2D) $S = 1$ isotropic Heisenberg model with a dimerized structure and frustrating interactions it was suggested an emergence of the spin supersolid state (a long-range mixing of superfluid and charge ordered phases) induced by a magnetic field.[11]

The organic compound F_2PNNNO is a supplementary example of spin-one dimer based magnetic insulator. This is 2D Heisenberg system with a singlet ground state, in which $S = 1$ dimers interact antiferromagnetically.[12,13] The lattice of the system is equivalent to the honeycomb one (Fig. 1). The field magnetization process shows a two-step saturation behavior that is a rare example of observation of a plateau in a two-dimensional system. The intermediate plateau corresponds to the half value of saturation magnetization. The consistent calculation of susceptibility and magnetization for the finite-size cluster with imposed periodic conditions yields the following estimations of antiferromagnetic exchange couplings $2J_0 = 67.5$ K, $2J_1 = 7.5$ K, i.e. the system can be regarded as a real 2D dimerized spin-one system.

Apparently, the quantum antiferromagnet F_2PNNNO offers an opportunity to verify a relevance of semi-hard core boson model for description of the dimerized system. In the paper we perform a diagonalization of finite cluster of $N = 18$ sites, calculate the magnetization and demonstrate that these results can be easily understood within the semi-hard boson model with strong on-site and inter-site repulsions. The diagonalization procedure used by us accounts the spin rotational symmetry.[14,15] The implementation of non-Abelian $SU(2)$ spin symmetry is based on an elimination of quantum numbers via the Wigner-Eckart theorem. The advantage of the approach is that the cluster spin states are decomposed into different sectors of the total cluster spin. In addition, one can independently handle each of the target spin state.

The paper is organized as follows. The model and the diagonalization algorithm are given in Sec.II. The truncation procedure is discussed in Sec.III. In Sec.IV we report numerical cluster calculations of the spectrum and the magnetization curve. The analogy with the lattice boson model is performed in Sec.V. Main results are recapitulated in the Conclusion part.

II. THE MODEL

The Hamiltonian of weakly interacting spin-one dimers on a 2D lattice depicted in Fig. 1 is given by

$$H_S = J_0 \sum_i \vec{S}_{i1}\vec{S}_{i2} + J_1 \sum_{\langle i\alpha, j\bar{\alpha}\rangle} \vec{S}_{i\alpha}\vec{S}_{j\bar{\alpha}}, \tag{1}$$

where J_0 is the coupling inside the i-th dimer, J_1 is the strength of the exchange interaction between the dimers located on the bonds $\langle i, j\rangle$. The indices α, $\bar{\alpha}$ mark $S = 1$ spins that enter into the interacting dimers, namely, $\bar{\alpha}$ = 1,2 provided α = 2,1, respectively. The both types of the interactions are antiferromagnetic $J_{0,1} > 0$, and the regime of weakly interacting dimers, $|J_0| \gg |J_1|$, is considered. The Heisenberg model has been previously suggested to explain some thermodynamical properties of F_2PNNNO.[12] Numerical calculations based on the Hamiltonian (1) via exact diagonalization of small clusters and their comparison with experimental data prove its relevance for the ratio $|J_1/J_0| \ll 1$. The dimerization caused by the anisotropy of interactions on a lattice is somewhat analogous to a situation in two-leg spin-1 antiferromagnetic ladders in a strong antiferromagnetic rung-coupling regime, when the ladder ground state is well approximated by the tensor product of singlet rung-dimers.[16]

To get the energy spectrum the finite-size clusters composed of $N = 10$ and $N = 18$ sites are selected. In a choice of the cluster care should be taken to ensure that the lattice point group symmetry is hold. Since intra-dimer interactions are the strongest, the cluster should consist of intact dimers. To mark sites inside the cluster the chessboard-like notations will be used, i.e. site positions along the x axis are marked by numbers whereas positions along the y axis are denoted by Latin letters.

To find eigenfunctions of the cluster that inherit the total cluster spin as a quantum number we should develop a consecutive procedure of addition of spin moments. It is convenient to break the cluster in several parts. Following the strategy of a cluster building used in Ref.[15], one should identify the central dimer (center) and its environment. The center is composed of the $c3$ and $d3$ sites whereas another sites are embodied into the environment.

The Hamiltonian of the central dimer has the form $H_c = J_0\vec{S}_{c3}\vec{S}_{d3}$, whereas the interaction between the center and its environment is given by

$$V_{\rm ce} = J_1\vec{S}_{c3}\left(\vec{S}_{c2} + \vec{S}_{c4}\right) + J_1\vec{S}_{d3}\left(\vec{S}_{d2} + \vec{S}_{d4}\right). \tag{2}$$

The environment consists of four parts, namely of two dimers, left (l) and right (r) ones, with the Hamiltonians

$$H_l = J_0\vec{S}_{c1}\vec{S}_{d1}, \text{ and } H_r = J_0\vec{S}_{c5}\vec{S}_{d5}, \tag{3}$$

respectively, as well as two fork-like parts, i.e. the down and upper ones, with the corresponding Hamiltonians

$$H_{\rm down} = J_0\left(\vec{S}_{b2}\vec{S}_{c2} + \vec{S}_{a3}\vec{S}_{b3} + \vec{S}_{b4}\vec{S}_{c4}\right) + J_1\vec{S}_{b3}\left(\vec{S}_{b2} + \vec{S}_{b4}\right), \tag{4}$$

$$H_{\rm up} = J_0\left(\vec{S}_{d2}\vec{S}_{e2} + \vec{S}_{e3}\vec{S}_{f3} + \vec{S}_{d4}\vec{S}_{e4}\right) + J_1\vec{S}_{e3}\left(\vec{S}_{e2} + \vec{S}_{e4}\right). \tag{5}$$

The interaction between the left/right dimers and the fork-like parts is presented as

$$V_{\rm env} = J_1\left(\vec{S}_{c2}\vec{S}_{c1} + \vec{S}_{d2}\vec{S}_{d1} + \vec{S}_{c4}\vec{S}_{c5} + \vec{S}_{d4}\vec{S}_{d5}\right). \tag{6}$$

The Hamiltonian of the entire cluster gathers all the above terms

$$H = H_c + V_{\rm ce} + \{H_l + H_r + H_{\rm down} + H_{\rm up} + V_{\rm env}\}. \tag{7}$$

There are three states of the dimer, which is the elementary block of the cluster, with the total spin $S_{\rm dm} = 0$ (singlet), $S_{\rm dm} = 1$ (triplet), and $S_{\rm dm} = 2$ (quintiplet). The energies of the states are $E_0 = -2J_0$, $E_1 = -J_0$, $E_2 = J_0$, respectively, and the eigenstates are obtained via the common rule of addition of moments

$$|11; S_{\rm dm}M_{\rm dm}\rangle \equiv |S_{\rm dm}M_{\rm dm}\rangle = \sum_{\sigma_1\sigma_2} \begin{bmatrix} 1 & 1 & S_{\rm dm} \\ \sigma_1 & \sigma_2 & M_{\rm dm} \end{bmatrix} |1\sigma_1\rangle\,|1\sigma_2\rangle\,, \tag{8}$$

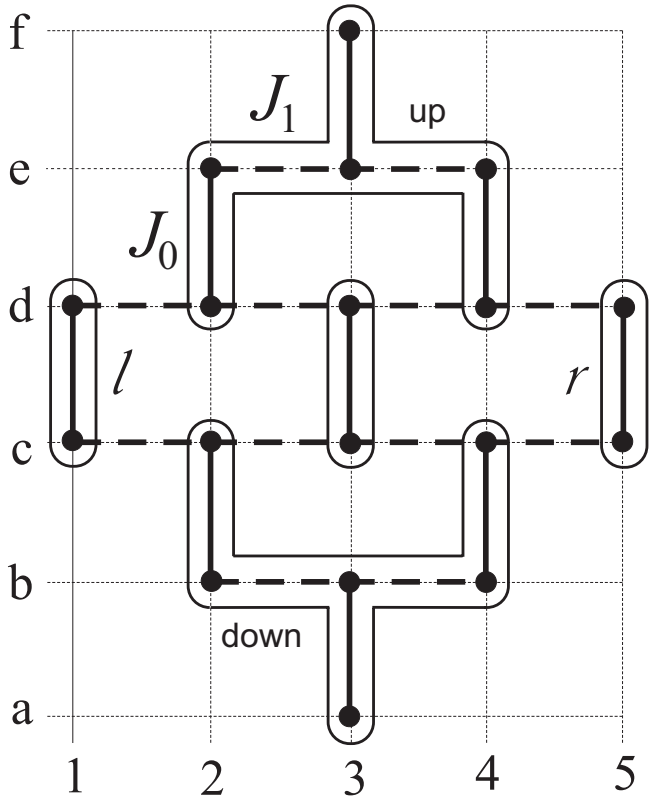

FIG. 1: The 18-site cluster used in numerical calculations. The environment of the central dimer consists of two "fork"-like parts (up and down), and the left (l) and right (r) dimers. The intra-dimer J_0 and inter-dimer J_1 interactions are shown by solid and dotted lines, respectively.

where [...] is the Clebsch-Gordan coefficient. To increase the cluster size the reduced matrix elements (RME) of the spin operators $S(1)$ and $S(2)$, that constitute the dimer, calculated within the basis (8) are needed

$$\left\langle S_{\rm dm} \left\| S(1) \right\| S'_{\rm dm} \right\rangle = (-1)^{1+S'_{\rm dm}} \sqrt{(2S_{\rm dm}+1)(2S'_{\rm dm}+1)} \left\{ \begin{array}{ccc} S_{\rm dm} & 1 & S'_{\rm dm} \\ 1 & 1 & 1 \end{array} \right\} \langle 1 \left\| S \right\| 1 \rangle \,, \tag{9}$$

$$\left\langle S_{dm} \left\| S(2) \right\| S'_{dm} \right\rangle = (-1)^{1+S_{dm}} \sqrt{(2S_{dm}+1)(2S'_{dm}+1)} \left\{ \begin{array}{ccc} S_{dm} & 1 & S'_{dm} \\ 1 & 1 & 1 \end{array} \right\} \langle 1 \left\| S \right\| 1 \rangle \,, \tag{10}$$

where $\{\ldots\}$ is the $6j$-symbol of the rotation group, and the reduced matrix element $\langle 1 \left\| S \right\| 1 \rangle = \sqrt{6}$.

The fork-like part includes three interacting dimers. It is convenient to build the basis of the fragment according to the scheme $(2+4)+3$ of the moment addition, i.e. a combining of the "prong" dimer functions is followed by adding of the "handle" function. As a result, the basic functions with the total spin $S_{\rm down}$ of the down fork-like part has the form

$$|(S_2 S_4)\, S_{24}, S_3; S_{\rm down} M_{\rm down}\rangle = \sum_{M_2 M_3 M_4 M_{24}} \left[\begin{array}{ccc} S_2 & S_4 & S_{24} \\ M_2 & M_4 & M_{24} \end{array} \right] \left[\begin{array}{ccc} S_{24} & S_3 & S_{\rm down} \\ M_{24} & M_3 & M_{\rm down} \end{array} \right] |S_2 M_2\rangle\, |S_3 M_3\rangle\, |S_4 M_4\rangle \,, \tag{11}$$

where S_2, S_3 and S_4 are the spins of the dimers composed of the $b2$ and $c2$ sites, etc. Within the basis the Hamiltonian (4) is presented by the block diagonal 141×141 matrix. The blocks are marked by the total spin $S_{\rm down} = 0, 1, \ldots, 6$ values. A diagonalization of the $H_{\rm down}$ matrix yields the spectrum $E_{i_{\rm down} S_{\rm down}}$ and the eigenfunctions

$$|i_{\rm down} S_{\rm down} M_{\rm down}\rangle = \sum_{S_2 S_3 S_4 S_{24}} \alpha^{i_{\rm down} S_{\rm down}}_{(S_2 S_4) S_{24}, S_3} \, |(S_2 S_4)\, S_{24}, S_3; S_{\rm down} M_{\rm down}\rangle \,,$$

where the index $i_{\rm down}$ distinguishes basic functions with the same total $S_{\rm down}$ spin. The results for the upper fork-like part can be obtained analogously provided the site $c4$ is substituted for $d2$, and $c2$ is changed by $d4$ etc. The assembly of the cluster part is completed by calculations of the reduced matrix elements [see Eq.(A1) in Appendix].

As the next step, we construct the spin functions of the non-interacting parts, i.e. of the left and the right dimers

$$|S_l S_r; S_{lr} M_{lr}\rangle = \sum_{M_l M_r} \left[\begin{array}{ccc} S_l & S_r & S_{lr} \\ M_l & M_r & M_{lr} \end{array} \right] |S_l M_l\rangle \, |S_r M_r\rangle \,, \tag{12}$$

where $S_{lr} = 0, 1 \ldots, 4$, and the upper and down fork-like parts

$$|i_{\rm up} S_{\rm up} i_{\rm down} S_{\rm down}; S_{\rm ud} M_{\rm ud}\rangle = \sum_{M_{\rm up} M_{\rm down}} \left[\begin{array}{ccc} S_{\rm up} & S_{\rm down} & S_{\rm ud} \\ M_{\rm up} & M_{\rm down} & M_{\rm ud} \end{array} \right] |i_{\rm up} S_{\rm up} M_{\rm up}\rangle \, |i_{\rm down} S_{\rm down} M_{\rm down}\rangle \,, \tag{13}$$

where $S_{\rm ud} = 0, 1 \ldots, 12$, and add them together to build the basis of the environment of the central dimer

$$|(i_{\rm up} S_{\rm up} i_{\rm down} S_{\rm down})\, S_{\rm ud}, (S_l S_r)\, S_{lr}; S_{\rm env} M_{\rm env}\rangle$$

$$= \sum_{M_{\rm ud} M_{lr}} \left[\begin{array}{ccc} S_{\rm ud} & S_{lr} & S_{\rm env} \\ M_{\rm ud} & M_{lr} & M_{\rm env} \end{array} \right] |i_{\rm up} S_{\rm up} i_{\rm down} S_{\rm down}; S_{\rm ud} M_{\rm ud}\rangle \, |S_l S_r; S_{lr} M_{lr}\rangle \,. \tag{14}$$

The reduced matrix elements of spin operators needed to build the Hamiltonian of the environment are relegated to Appendix [see Eqs.(A2-A5)]. Note, that a number of the states (14) is too much to avoid the truncation procedure (see Sec.III).

Matrix elements of the environment Hamiltonian $H_{\rm env} = H_l + H_r + H_{\rm down} + H_{\rm up} + V_{\rm env}$ are given as follows

$$\left\langle (i_{\rm up} S_{\rm up} i_{\rm down} S_{\rm down})\, S_{\rm ud}, (S_l S_r)\, S_{lr}; S_{\rm env} M_{\rm env} | H_{\rm env} | \left(i'_{\rm up} S'_{\rm up} i'_{\rm down} S'_{\rm down}\right) S'_{\rm ud}, (S'_l S'_r)\, S'_{lr}; S'_{\rm env} M'_{\rm env} \right\rangle$$

$$= \left(E_{i_{\rm up} S_{\rm up}} + E_{i_{\rm down} S_{\rm down}} + E_{S_l} + E_{S_r}\right) \delta_{i_{\rm up}, i'_{\rm up}} \delta_{S_{\rm up}, S'_{\rm up}} \delta_{i_{\rm down}, i'_{\rm down}} \delta_{S_{\rm down}, S'_{\rm down}} \delta_{S_{\rm ud}, S'_{\rm ud}} \delta_{S_l, S'_l} \delta_{S_r, S'_r} \delta_{S_{lr}, S'_{lr}} \delta_{S_{\rm env}, S'_{\rm env}} \delta_{M_{\rm env}, M'_{\rm env}}$$

$$+ J_1 \delta_{S_{\rm env}, S'_{\rm env}} (-1)^{S_{\rm env} + S'_{\rm ud} + S_{lr}} \left\{ \begin{array}{ccc} S_{\rm ud} & S_{lr} & S_{\rm env} \\ S'_{lr} & S'_{\rm ud} & 1 \end{array} \right\} \delta_{M_{\rm env}, M'_{\rm env}} \tag{15}$$

$$\times \Big\{ \langle S_l S_r; S_{lr} \| S_{c1} \| S'_l S'_r; S'_{lr} \rangle \left\langle i_{\rm up} S_{\rm up} i_{\rm down} S_{\rm down}; S_{\rm ud} \| S_{c2} \| i'_{\rm up} S'_{\rm up} i'_{\rm down} S'_{\rm down}; S'_{\rm ud} \right\rangle$$

$$+ \langle S_l S_r; S_{lr} \| S_{d1} \| S'_l S'_r; S'_{lr} \rangle \left\langle i_{\rm up} S_{\rm up} i_{\rm down} S_{\rm down}; S_{\rm ud} \| S_{d2} \| i'_{\rm up} S'_{\rm up} i'_{\rm down} S'_{\rm down}; S'_{\rm ud} \right\rangle$$

$$+ \langle S_l S_r; S_{lr} \| S_{c5} \| S'_l S'_r; S'_{lr} \rangle \left\langle i_{\rm up} S_{\rm up} i_{\rm down} S_{\rm down}; S_{\rm ud} \| S_{c4} \| i'_{\rm up} S'_{\rm up} i'_{\rm down} S'_{\rm down}; S'_{\rm ud} \right\rangle$$

$$+ \langle S_l S_r; S_{lr} \| S_{d5} \| S'_l S'_r; S'_{lr} \rangle \left\langle i_{\rm up} S_{\rm up} i_{\rm down} S_{\rm down}; S_{\rm ud} \| S_{d4} \| i'_{\rm up} S'_{\rm up} i'_{\rm down} S'_{\rm down}; S'_{\rm ud} \right\rangle \Big\} \,.$$

The terms in $\{\ldots\}$ include product of the reduced matrix elements given by Eqs.(A2,A3) for spins that enter into the left/right dimers and by Eq.(A4,A5) for the constituents of the fork-like parts.

After a finding of the environment eigenvalues $E_{i_{\rm env} S_{\rm env}}$ and eigenfunctions

$$|i_{\rm env} S_{\rm env} M_{\rm env}\rangle = \sum \beta^{i_{\rm env} S_{\rm env}}_{(i_{\rm up} S_{\rm up} i_{\rm down} S_{\rm down}) S_{\rm ud}, (S_l S_r) S_{lr}} \, |(i_{\rm up} S_{\rm up} i_{\rm down} S_{\rm down})\, S_{\rm ud}, (S_l S_r)\, S_{lr}; S_{\rm env} M_{\rm env}\rangle \,, \tag{16}$$

one calculate within the basis the reduced matrix elements for the environment spins that directly interact with the central dimer see [Eq.(A6)].

At the final step of the diagonalization procedure one build the basis of the entire cluster

$$|i_{\rm env} S_{\rm env}, S_c; S M\rangle = \sum_{M_{\rm env} M_c} \left[\begin{array}{ccc} S_{\rm env} & S_c & S \\ M_{\rm env} & M_c & M \end{array} \right] |i_{\rm env} S_{\rm env} M_{\rm env}\rangle \, |S_c M_c\rangle \,,$$

and determine the matrix elements of the cluster Hamiltonian (7)

$$\langle i_{\rm env} S_{\rm env}, S_c; S M | H | i'_{\rm env} S'_{\rm env}, S'_c; S' M' \rangle = \left(E_{i_{\rm env} S_{\rm env}} + E_{S_c}\right) \delta_{i_{\rm env}, i'_{\rm env}} \delta_{S_{\rm env}, S'_{\rm env}} \delta_{S_c, S'_c} \delta_{S, S'} \delta_{M, M'}$$

$$+J_1\,(-1)^{S+S'_{\rm env}+S_c}\left\{\begin{array}{ccc} S_{\rm env} & S_c & S \\ S'_c & S'_{\rm env} & 1 \end{array}\right\}\delta_{S,S'}\delta_{M,M'}$$

$$\times\left[\langle S_c\,\|S(1)\|\,S'_c\rangle\sum_{k=c2,c4}\langle i_{\rm env}S_{\rm env}\,\|S_k\|\,i'_{\rm env}S'_{\rm env}\rangle+\langle S_c\,\|S(2)\|\,S'_c\rangle\sum_{k=d2,d4}\langle i_{\rm env}S_{\rm env}\,\|S_k\|\,i'_{\rm env}S'_{\rm env}\rangle\right], \qquad (17)$$

where the RMEs are previously derived [see Eqs.(9-10) and Eq.(A6)]. Numerical diagonalization of the matrix (17) yields the target spectrum E_{iS} and the eigenfunctions

$$|iSM\rangle=\sum\gamma^{iS}_{S_{\rm env}M_{\rm env},S_c}\,|S_{\rm env}M_{\rm env},S_c;SM\rangle\,. \qquad (18)$$

III. TRUNCATION PROCEDURE

The classification of eigenstates of parts used to gather the total cluster according to irreducible representations of $SU(2)$-group enables to organize a truncation procedure inside the sectors of Hilbert space that arise at the consecutive steps of the algorithm. A possibility to carry out calculations within a reduced basis is feature of the algorithm that relates it with other renormalization group methods.

We hold the following strategy of the truncation procedure to build target states that are obtained after combining two parts of the lattice. For a given spin-S sector a certain amount of states having the lowest energy are kept. Thus every group of the $|iS\rangle$ states is presented in the reduced basis. We truncate the basis of two "fork"-like parts before to combine them into a larger lattice segment. This is not the unique way, for example one can truncate the basis of the environment after combining the "fork"-like parts, but the former is easier to perform.

We tested several realizations of the truncation procedure either by simply controlling a number of vectors retained in the reduced basis or by monitoring a genealogy of the target spin-S state through the triangle rule, i.e. only states that contribute into the target state are took into account. The last approach gives an opportunity to keep more vectors in the basis due to an omitting of redundant states. Moreover, highest-spin cluster states, i.e. those with $S\geq 15$ in our problem, are treated exactly. The size of truncated basis was chosen to be equal to either 64 or 121 for the scheme without an account of genealogy of the target state, and it varies from 12 till 352, being depending on the total spin S, for the "genealogical" scheme.

An accuracy of the truncation procedure is controlled by monitoring an energy of the lowest state within an each spin sector. The variation of this observable computed through the both schemes does not usually exceed 1-2% (a maximal discrepancy of order 6% is reached only in the S-8 sector) that evidences a correctness of the constructed basis which exhibits almost no dependence on the used truncation procedure. The results that we present below are obtained within the "genealogical" scheme.

Another feature of the algorithm is an addition of a central unit (one site or dimer) with its environment at the final step. The procedure does not depend on a structure of the environment and looks similar for any cluster. However, the information about quantum numbers of the environment states enables to simplify calculations substantially at the stage of the algorithm. Indeed, for a given spin-S sector of the Hilbert space of the entire cluster one should pick out only those environment eigenfunctions whose spins S_u obey the rule

$$|S_u-S_c|\leq S\leq S_u+S_c.$$

Using of the truncation procedure results in the basises composed maximally from 4-5 thousand states. To control an accuracy of the procedure the results obtained for the 18-site system are compared with those for 10-site system. The smaller cluster enables to handle a whole basis without any truncation. The 10-site system is embedded into the bigger cluster and consists of the following parts: the central dimer $c3, d3$ and the neighbor dimers $b2, c2$, $b4, c4$, $d2, e2$ and $d4, e4$. Apparently, a construction of the environment requires two consecutive steps (i) an addition of the dimers $b2, c2$ and $b4, c4$ as well as $d2, e2$ and $d4, e4$ ones according to Eq.(12) then followed by a calculation of reduced matrix elements according to Eq.(A2,A3); (ii) a construction of the environment states from the upper and down parts built previously and a calculation of RME of the environment spins that interact directly with the central dimer. The entire cluster Hamiltonian is obtained through (17). The biggest Hilbert space dimension (2025×2025) is reached in the S-2 sector. The numerical results for the supplementary cluster are listed in Table I for comparison. Note that one should compare energy values with the same magnetization per dimer (See Fig. 2).

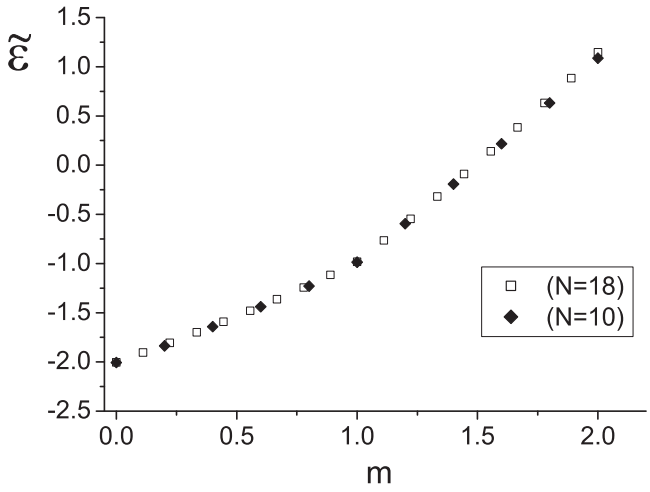

FIG. 2: Plot of the lowest energy per dimer $\tilde{\varepsilon}\,(m)$ vs m for the $N = 10$ and $N = 18$ clusters. The cusp is seen at $m = 1$.

IV. ENERGY SPECTRUM AND MAGNETIZATION CURVE

The results of the energy spectrum calculation for two $N = 10$ and $N = 18$ clusters are listed in Table I, where we give minimal energy $E_{\min}$ within the each spin-S sector along with the energy per dimer $\tilde{\varepsilon} = 2E_{\min}/N$. The magnetization per dimer is determined by $m = 2S/N$. The $N = 10$ and $N = 18$ dependencies $\tilde{\varepsilon}\,(m)$ are shown together in Fig. 2. The points for both clusters lay on one curve, i.e. finite-size effects may be ignored that is expected for the regime of a small dimer-dimer interaction $J_1 \ll J_0$.

A remarkable feature of the curve is a cusp in the middle, i.e. at $m = 1$. The independent fitting of both parts jointed in the point by the quadratic form $\varepsilon(m) = \varepsilon_2 m^2 + \varepsilon_1 m + \varepsilon_0$ yields $\varepsilon_2 = 0.190 \pm 0.018$, $\varepsilon_1 = 0.828 \pm 0.019$, and $\varepsilon_0 = -2.0073 \pm 0.0040$ for the lower part of the curve ($0 < m < 1$) together with $\varepsilon_2 = 0.200 \pm 0.058$, $\varepsilon_1 = 1.4578 \pm 0.018$, and $\varepsilon_0 = -2.629 \pm 0.014$ for the upper part ($1 < m < 2$).

On the base of data for N=18 case we build a dependence of jumps $E_{\min}$ when the total spin S changes from 0 till 18, or the dimer magnetization varies from 0 till 2 (Fig. 3) One can see that the values of the jumps are approximately J_0 for $S \leq 9$ and they are increased by a factor of 2 as $S \geq 10$. It means that the energy of the total system of weakly interacting dimers will change with an increasing magnetic field due to local excitations inside separate dimers. Indeed, for the single $S = 1$ dimer the spectrum consists of a singlet, a triplet, and a quintuplet. The energy difference between the singlet and triplet is J_0 while the difference between the quintuplet and the triplet is $2J_0$ (see discussion in the next Section).

A standard way to consider a magnetization process at $T = 0$ is to define $E^{(S)}_{\min}(N)$ as the lowest energy of the Hamiltonian (1) in the spin-S subspace for a finite system of N elementary dimers. Applying a magnetic field B leads to a Zeeman splitting of the energy levels $E^{(S)}_{\min}(B) = E^{(S)}_{\min} - SB$, and therefore level crossing occurs at values $B_S = E^{(S+1)}_{\min}(B) - E^{(S)}_{\min}(B)$ when increasing the field. These level crossings correspond to jumps in the magnetization at zero temperature of the value $1/N$, until the fully polarized state with the magnetization per dimer $m_{\rm sat} = 2N/N = 2$ is reached at the value of the magnetic field $B_{\rm sat} = E^{(2N)}_{\min}(B) - E^{(2N-1)}_{\min}(B)$. The calculation performed for $N/2 = 9$ dimers yields the magnetization points presented in Fig. 4 and demonstrates an appearance of the ground state plateau as well as the plateau at one-half of the saturation value.

To guarantee a validity of the magnetization curve we use an approach developed by Sakai and Tahakashi[17] to recover the $m(B)$ dependence in the thermodynamical limit. In this case the condition for the crossover fields transforms into $B = \varepsilon'(m)$, where ε is the energy per dimer. The plateau boundaries are determined by the derivatives in the special points: (i) $B_1 = \varepsilon'(+0)$ is related with the end of the ground state plateau; (ii) $B_2 = \varepsilon'(1-0)$ and $B_3 = \varepsilon'(1+0)$ correspond to the beginning and the end of the intermediate plateau, respectively; (iii) $B_4 = \varepsilon'(2-0)$ marks an emergence of the saturation magnetization.

A treatment of the energy spectrum results in the linear dependences relevant for sectors between the plateaus

$$\begin{cases} \varepsilon'(m) = 0.83 + 0.38\,m, \ 0 < m < 1, \\ \varepsilon'(m) = 1.46 + 0.40\,m, \ 1 < m < 2, \end{cases} \tag{19}$$

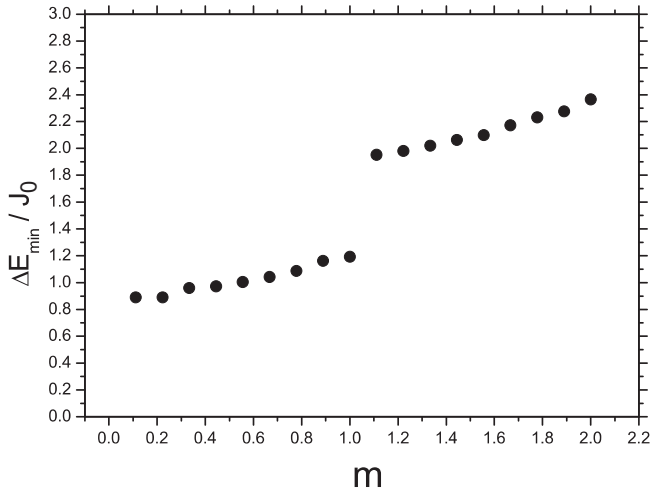

FIG. 3: Plot of the changes $\Delta E_{\min}$ versus the dimer magnetization m. A distinct jump is seen at $m = 1$.

TABLE I: Numerical results of the lowest energy $E_{\min}$ and the energy $\tilde{\varepsilon}$ per dimer in the spin-S subspaces for $N = 10$ and $N = 18$ clusters.

S	$E_{\min}(N=10)/J_0$	$\tilde{\varepsilon}\,(N=10)$	$E_{\min}(N=18)/J_0$	$\tilde{\varepsilon}\,(N=18)$
0	−10.0334	−2.0067	−18.0336	−2.0037
1	−9.1853	−1.8371	−17.1431	−1.9048
2	−8.2123	−1.6425	−16.2529	−1.8059
3	−7.1978	−1.4396	−15.2935	−1.6993
4	−6.1430	−1.2286	−14.3205	−1.5912
5	−4.9344	−0.9869	−13.3164	−1.4796
6	−2.9787	−0.5957	−12.2745	−1.3638
7	−0.9610	−0.1922	−11.1879	−1.2431
8	1.0849	0.2170	−10.0260	−1.1140
9	3.1588	0.6318	−8.8335	−0.9815
10	5.4418	1.0883	−6.8807	−0.7645
11			−4.8994	−0.5444
12			−2.8795	−0.3199
13			−0.8172	−0.0908
14			1.2815	0.1424
15			3.4533	0.3837
16			5.6844	0.6316
17			7.960	0.8844
18			10.3254	1.1473

that produces immediately $B_1 = 0.83\,J_0$, $B_2 = 1.21\,J_0$, $B_3 = 1.86\,J_0$, and $B_4 = 2.26\,J_0$. The values normalized to the saturation field $B_{\rm sat}$ are listed in the Table II and exhibit a reasonable agreement with the experimental data for F_2PNNNO system. A comparison of the finite cluster calculations with those of the thermodynamical limit (19) is given in Fig. 4. It is seen that both methods produce the close results.

Note that the method we used for numerical calculations is intrinsically two-dimensional one whereas the previous numerical study of the system[12] dealt with the cluster embedded into a chain. The regions between the plateaus of the magnetization curve exhibit a behavior closer to linear one instead of the S-shape forms early obtained.

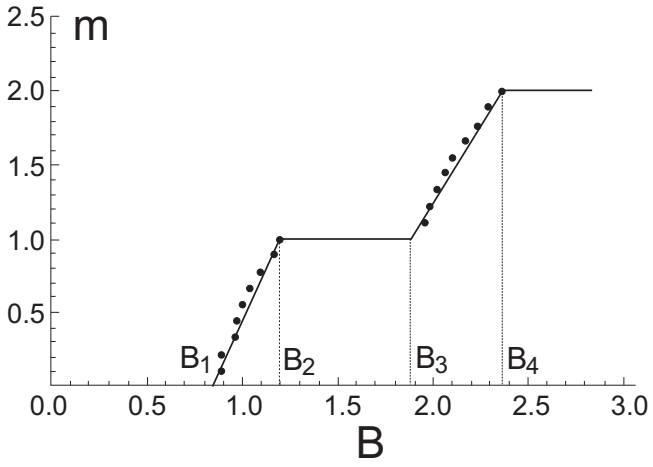

FIG. 4: Plot of m versus B obtained via $B = \varepsilon'(m)$. The dots mark values found through the diagonalization algorithm.

TABLE II: Values of the magnetic field special points compared with the experimental data.

$B_i/B_{\rm sat}$	$i=1$	$i=2$	$i=3$	$i=4$
Theory	0.37	0.53	0.82	1
Experiment[12]	0.33	0.53	0.89	1

V. SEMI-HARD CORE BOSON MODEL

Let us introduce the boson picture on the base of data presented in Fig. 3. For $J_1 \ll J_0$ the low energy subspace of spin Hamiltonian (1) consists of the singlet, the $S^z = 1$ component of the triplet, and the $S^z = 2$ component of the quintuplet. It is convenient to identify the triplet state with a presence of a bosonic particle (triplon), the quintiplet state as a pair of bosons (quintuplon), and the singlet state as an absence of bosons. Then the boson model is formulated via the semi-hard core bosonic operators g_i and $g_i^\dagger$ with the extended Pauli's exclusion principle ${g_i^\dagger}^3 = 0$, i.e. more then two bosons per site are forbidden. Note that the principle may be realized via parafermion language but the description requires a transmutation of statistics that complicates calculations in a 2D case (see Appendix B). The algebra of the operators are $[g_i, g_i] = \left[g_i^\dagger, g_i^\dagger\right] = 0$, and $\left[g_i, g_i^\dagger\right] = \delta_{ij}\,(1 - F_i)$, where $F_i = (3/2)\,n_i\,(n_i - 1)$ is the deformation of the canonical boson algebra, $n_i = g_i^\dagger g_i$ is the number operator.[10]

The boson Hamiltonian in terms of these operators is written as

$$H = \frac{1}{2}\sum_{\langle ij\rangle}\left(g_i^\dagger g_j + g_j^\dagger g_i\right)(h_1 + h_2 + h_3) - \mu\sum_i n_i + \frac{U}{2}\sum_i n_i\,(n_i + 1) + V\sum_{\langle ij\rangle}(n_i - 1)\,(n_j - 1)\,, \tag{20}$$

where the hopping terms

$$h_1 = t_1\,(n_{ij} - 2)\,(n_{ij} - 3)\,,\ h_2 = 2t_2\,(n_{ij} - 1)\,(3 - n_{ij})\,,\ h_1 = t_3\,(n_{ij} - 1)\,(n_{ij} - 2)$$

depend on a number of particles $n_{ij} = n_i + n_j$ on the bonds i, j.

The map between the bosonic (20) and the spin Hamiltonian (1) is reached through the representation[11] (see Fig. 5)

$$n_i = S_i^z = S_{i1}^z + S_{i2}^z,$$

where $(1, 2)$ marks two spins on each dimer, and

$$g_i^\dagger = \frac{1}{\sqrt{2}}\left(S_{i2}^\dagger - S_{i1}^\dagger\right)\left[\frac{\sqrt{3}}{2\sqrt{2}} + \left(1 - \frac{\sqrt{3}}{2\sqrt{2}}\right)S_i^z\right].$$

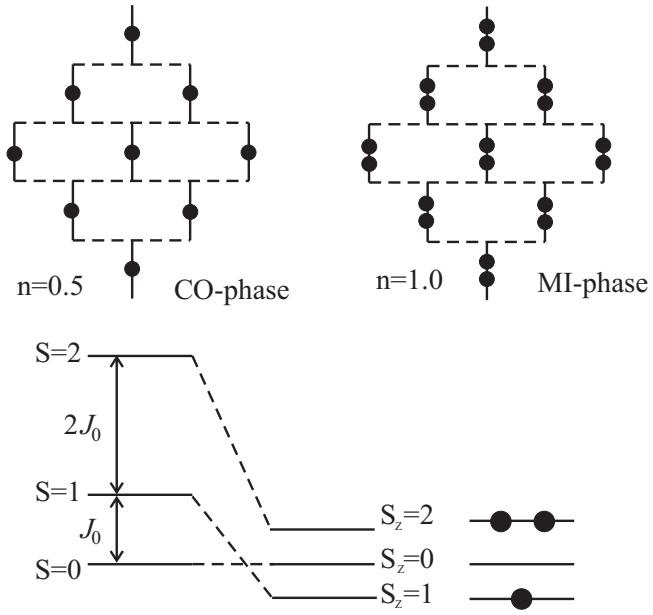

FIG. 5: The low energy subspace of the single dimer spectrum in the presence of a magnetic field. Boson superlattice patterns corresponding to the charge-ordered and Mott insulating phases are shown above.

This establishes the relationship between the spin and the bosonic parameters $U = J_0$, $V = J_1/2$, $\mu = B - 4J_1$, and $t_i = -\frac{8\sqrt{2}}{3\sqrt{3}} a^i J_1$, where $a = \frac{\sqrt{3}}{2\sqrt{2}}$ $(i = 1, 2, 3)$. Thus, the bosonic model includes the strong on-site boson repulsion U as well as the noticeable repulsive intersite interaction V. The magnetic field B plays the role of the chemical potential μ.

The boson Hamiltonian (20) constitutes low-energy effective model of the spin Hamiltonian (1) that appears from restricting H_S to the subspace of the semi-hard core bosonic operators. The map is valid in the limit $J_1 \ll J_0$, or in the boson language t_i/U, $V/U \ll 1$, when the main physics is governed by a competition between the one-site repulsion and the chemical potential.

The quantum phase diagram of the boson Hamiltonian (20) was built in Ref.[11] by using the stochastic series expansion quantum Monte Carlo method (see there Fig.4). It has been found that a Bose condensate fraction appears in the regions of the chemical potential (magnetic field) between the platos of the g-particles density (magnetization curve). In contrast, the charge density wave (Ising-like charge order (CO) phase) forms around the intermediate plato. There are regions, where supersolid phase, a mixing of the charge order and the Bose-supefluid (BS), emerges. According to the study the magnetization curve shown in Fig. 4 can be interpreted as a tuning of boson density by the applied magnetic field. At small chemical potential the empty states has the lowest energy, when all dimers in the singlet state (boson vacuum). For $B > B_1$ a finite density of bosons (triplons) emerges in the ground state and contributes into a BS phase. The triplon excitations are mobile due to weak interdimer coupling. The density (magnetization) increases monotonically as a function of magnetic field until B_2, where a transition to the CO-phase comes up. This corresponds to the boson concentration $n = 0.5$, when the triplons crystallize in a superstructure pattern (Fig. 5). The fractional plateau requires strong boson interactions in comparison to the kinetic energy. At $B > B_3$ the filling increases monotonically in the resulting BS phase (quintiplon condensation) till the ground state transforms into a Mott insulating (MI) phase with two bosons per dimer at $B > B_4$. The boson concentration in the MI phase $n = 1$. The reasonings are easily reproduced if to analyze the boson Hamiltonian (20) by neglecting the intersite terms.

VI. CONCLUSIONS

Quantum dimer antiferromagnetic systems is a nice testing area to study BEC of interacting particles. Along with the ultracold atomic gases in optical lattices[18,19] they offer an opportunity to observe transitions predicted by lattice boson models. In many problems the boson picture is more physically transparent than the original spin language. On the base of the analysis of the finite cluster energy spectrum for the two-dimensional spin-1 organic antiferromagnet

F_2PNNNO with the dimerized structure we prove a relevance of the model of semi-hard core bosons with pronounced on-site and inter-site repulsions for the low-dimensional spin system. The unusual magnetization curve observed in F_2PNNNO is nothing but a manifestation of fine-tune of density of the bosons by the applied magnetic field, when the low-density Bose-superfluid, charge ordering with one boson per a dimer, and high-density Bose-supefluid phases change subsequently each other with an increasing of the field.

Acknowledgments

We would like to thank T. Sakai, J. Kishine and N.V. Baranov for discussions. V.E.S. would like to acknowledge the support of the U.S. Civilian Research & Development Foundation (CRDF) and Ministery of Education and Science of Russian Federation (MinES) under "Basic Research and Higher Education" (BRHE) program.

APPENDIX A

The reduced matrix elements for spins on the $c2$ and $c4$ sites computed in the basis of eigenfunctions of the Hamiltonian $H_{\rm down}$ are given by the 141×141 matrix

$$\left\langle i_{\rm down} S_{\rm down} \left\| S_{c2(c4)} \right\| i'_{\rm down} S'_{\rm down} \right\rangle = \sum_{S_2 S_3 S_4 S_{24}} \sum_{S'_2 S'_3 S'_4 S'_{24}} \alpha^{i_{\rm down} S_{\rm down}}_{(S_2 S_4) S_{24}, S_3} \alpha^{i'_{\rm down} S'_{\rm down}}_{(S'_2 S'_4) S'_{24}, S'_3}$$

$$\times \left\langle (S_2 S_4)\, S_{24}, S_3; S_{\rm down} \left\| S_{c2(c4)} \right\| (S'_2 S'_4)\, S'_{24}, S'_3; S'_{\rm down} \right\rangle . \tag{A1}$$

The reduced matrix elements that enter into the expression are calculated according to the rules

$$\langle (S_2 S_4)\, S_{24}, S_3; S_{\rm down} \| S_{c2} \| (S'_2 S'_4)\, S'_{24}, S'_3; S'_{\rm down} \rangle = (-1)^{S_2+S_4+S_3+S_{24}+S'_{24}+S'_{\rm down}} \left[S_{24}, S'_{24}, S_{\rm down}, S'_{\rm down} \right]^{1/2}$$

$$\times \left\{ \begin{array}{ccc} S_{24} & 1 & S'_{24} \\ S'_2 & S_4 & S_2 \end{array} \right\} \left\{ \begin{array}{ccc} S_{\rm down} & 1 & S'_{\rm down} \\ S'_{24} & S_3 & S_{24} \end{array} \right\} \langle 11; S_2 \| S(2) \| 11; S'_2 \rangle\, \delta_{S_4 S'_4} \delta_{S_3 S'_3},$$

$$\langle (S_2 S_4)\, S_{24}, S_3; S_{\rm down} \| S_{c4} \| (S'_2 S'_4)\, S'_{24}, S'_3; S'_{\rm down} \rangle = (-1)^{S_2+S'_4+S_3+2S_{24}+S'_{\rm down}} \left[S_{24}, S'_{24}, S_{\rm down}, S'_{\rm down} \right]^{1/2}$$

$$\times \left\{ \begin{array}{ccc} S_{24} & 1 & S'_{24} \\ S'_4 & S_2 & S_4 \end{array} \right\} \left\{ \begin{array}{ccc} S_{\rm down} & 1 & S'_{\rm down} \\ S'_{24} & S_3 & S_{24} \end{array} \right\} \langle 11; S_4 \| S(2) \| 11; S'_4 \rangle\, \delta_{S_2 S'_2} \delta_{S_3 S'_3},$$

where $[S] = (2S+1)$.

The reduced matrix elements for spins on the sites $c1$ ($d1$) are given by the 19×19 matrix built in the basis of functions constructed from the "left" and the "right" dimers Eq.(12)

$$\left\langle S_l S_r; S_{lr} \left\| S_{c1(d1)} \right\| S'_l S'_r; S'_{lr} \right\rangle = \sqrt{(2S_{lr}+1)(2S'_{lr}+1)} (-1)^{1+S_l+S_r+S'_{lr}} \left\{ \begin{array}{ccc} S_{lr} & 1 & S'_{lr} \\ S'_l & S_r & S_l \end{array} \right\} \langle 11; S_l \| S(1(2)) \| 11; S'_l \rangle\, \delta_{S_r S'_r}. \tag{A2}$$

The RME for spins on the $c5$ ($d5$) sites amount to

$$\left\langle S_l S_r; S_{lr} \left\| S_{c5(d5)} \right\| S'_l S'_r; S'_{lr} \right\rangle = \sqrt{(2S_{lr}+1)(2S'_{lr}+1)} (-1)^{1+S_l+S'_r+S_{lr}} \left\{ \begin{array}{ccc} S_{lr} & 1 & S'_{lr} \\ S'_r & S_l & S_r \end{array} \right\} \langle 11; S_r \| S(1(2)) \| 11; S'_r \rangle\, \delta_{S_l S'_l}. \tag{A3}$$

The reduced matrix elements of spin operators on sites $c2(d2), c4(d4)$ calculated on the eigenfuctions of the upper and down parts form the 73789×73789 matrices.

$$\left\langle i_{\rm up} S_{\rm up} i_{\rm down} S_{\rm down}; S_{\rm ud} \left\| S_{c2(c4)} \right\| i'_{\rm up} S'_{\rm up} i'_{\rm down} S'_{\rm down}; S'_{\rm ud} \right\rangle = \sqrt{(2S_{\rm ud}+1)(2S'_{\rm ud}+1)} (-1)^{1+S_{\rm up}+S'_{\rm down}+S_{\rm ud}}$$

$$\left\{ \begin{array}{ccc} S_{\rm ud} & 1 & S'_{\rm ud} \\ S'_{\rm down} & S_{\rm up} & S_{\rm down} \end{array} \right\} \left\langle i_{\rm down} S_{\rm down} \left\| S_{c2(c4)} \right\| i'_{\rm down} S'_{\rm down} \right\rangle \delta_{i_{\rm up} i'_{\rm up}} \delta_{S_{\rm up} S'_{\rm up}}. \tag{A4}$$

$$\left\langle i_{\rm up} S_{\rm up} i_{\rm down} S_{\rm down}; S_{\rm ud} \left\| S_{d2(d4)} \right\| i'_{\rm up} S'_{\rm up} i'_{\rm down} S'_{\rm down}; S'_{\rm ud} \right\rangle = \sqrt{(2S_{\rm ud}+1)(2S'_{\rm ud}+1)} (-1)^{1+S_{\rm up}+S_{\rm down}+S'_{\rm ud}}$$

$$\left\{ \begin{array}{ccc} S_{\rm ud} & 1 & S'_{\rm ud} \\ S'_{\rm up} & S_{\rm down} & S_{\rm up} \end{array} \right\} \left\langle i_{\rm up} S_{\rm up} \left\| S_{d2(d4)} \right\| i'_{\rm up} S'_{\rm up} \right\rangle \delta_{i_{\rm down} i'_{\rm down}} \delta_{S_{\rm down} S'_{\rm down}}. \tag{A5}$$

The reduced matrix elements of spin operators on sites $c2(d2), c4(d4)$ calculated on the eigenfuctions of the environment. The dimension of this matrices determines by dimension of truncated basis of environment

$$\langle i_{\rm env} S_{\rm env} \| S_k \| i'_{\rm env} S'_{\rm env} \rangle = \sum \beta^{i_{\rm env} S_{\rm env}}_{(i_{\rm up} S_{\rm up} i_{\rm down} S_{\rm down}) S_{\rm ud}, (S_l S_r) S_{lr}} \beta^{i'_{\rm env} S'_{\rm env}}_{\left(i'_{\rm up} S'_{\rm up} i'_{\rm down} S'_{\rm down}\right) S'_{\rm ud}, \left(S'_l S'_r\right) S'_{lr}}$$

$$\times \left\langle \left(i_{\rm up} S_{\rm up} i_{\rm down} S_{\rm down}\right) S_{\rm ud}, \left(S_l S_r\right) S_{lr}; S_{\rm env} \| S_k \| \left(i'_{\rm up} S'_{\rm up} i'_{\rm down} S'_{\rm down}\right) S'_{\rm ud}, \left(S'_l S'_r\right) S'_{lr}; S'_{\rm env} \right\rangle, \tag{A6}$$

where $k = c2(d2), c4(d4)$ and

$$\left\langle \left(i_{\rm up} S_{\rm up} i_{\rm down} S_{\rm down}\right) S_{\rm ud}, \left(S_l S_r\right) S_{lr}; S_{\rm env} \| S_k \| \left(i'_{\rm up} S'_{\rm up} i'_{\rm down} S'_{\rm down}\right) S'_{\rm ud}, \left(S'_l S'_r\right) S'_{lr}; S'_{\rm env} \right\rangle = \sqrt{(2S_{\rm env}+1)(2S'_{\rm env}+1)}$$

$$\times (-1)^{1+S_{\rm ud}+S_{lr}+S'_{\rm env}} \left\{ \begin{array}{ccc} S_{\rm env} & 1 & S'_{\rm env} \\ S'_{\rm ud} & S_{lr} & S_{\rm ud} \end{array} \right\} \left\langle i_{\rm up} S_{\rm up} i_{\rm down} S_{\rm down}; S_{\rm ud} \| S_k \| i'_{\rm up} S'_{\rm up} i'_{\rm down} S'_{\rm down}; S'_{\rm ud} \right\rangle \delta_{S_l S'_l} \delta_{S_r S'_r} \delta_{S_{lr} S'_{lr}}. \tag{A7}$$

APPENDIX B

Quantum statistics is based on two principles, the first is the exchange statistics, when a permutation of two identical particles causes an appearance of a phase factor in the total wave function, and the second is the exclusion statistics, which reflects an ability to accommodate p particles in the same single-particle quantum state. Whereas the first concept depends on the space dimensionality of the system, the second one does not.[20]

The exclusion statistics algebra obeying the generalized Pauli exclusion principle can be formulated in terms of the bond g operators that has been used in the main text. Another variant of the exclusion statistics can be realized, for example, via Green's parafermion statistics.[21,22] According to common formalism based on Burnside's theorem of the group theory (see Ref.[10] for details) the both algebraic approaches are related with each other.

Indeed, let us introduce two modes ($\alpha = 1, 2$) for the each i-th bond

$$\left\{ \begin{array}{c} \left\{ d_i^\alpha, d_j^\alpha \right\} = \left\{ \left(d_i^\alpha\right)^\dagger, \left(d_j^\alpha\right)^\dagger \right\} = 0, \\ \left\{ d_i^\alpha, \left(d_j^\alpha\right)^\dagger \right\} = \delta_{ij} \end{array} \right. \tag{B1}$$

with the condition $d_j^\alpha |\text{vacuum}\rangle = 0$. For $\alpha \neq \beta$ the modes satisfy non-standard relations

$$\left\{ \begin{array}{c} \left[d_i^\alpha, d_j^\beta \right] = \left[\left(d_i^\alpha\right)^\dagger, \left(d_j^\beta\right)^\dagger \right] = 0, \\ \left[d_i^\alpha, \left(d_j^\beta\right)^\dagger \right] = 0. \end{array} \right. \tag{B2}$$

Parafermion creation and annihilation operators are determined as

$$d_j^\dagger = \left(d_j^1\right)^\dagger + \left(d_j^2\right)^\dagger, \qquad d_j = d_j^1 + d_j^2. \tag{B3}$$

They satisfy the commutation relations

$$\left\{ \begin{array}{c} \left[\left[d_i^\dagger, d_j \right], d_l \right] = -2\delta_{il} d_j, \\ \left[\left[d_i, d_j \right], d_l \right] = 0. \end{array} \right. \tag{B4}$$

The parafermion number operator $n_j^d = \left(d_j^1\right)^\dagger d_j^1 + \left(d_j^2\right)^\dagger d_j^2$ can be written as

$$n_j^d = \frac{1}{2}\left(\left[d_i^\dagger, d_j\right] + 2\right), \tag{B5}$$

and obeys the commutation rule

$$\left[n_j^d, d_j^\dagger\right] = \delta_{ij} d_j^\dagger. \tag{B6}$$

From the property $\left(n_j^\alpha\right)^2 = n_j^\alpha$ it follows that n_j^d varies from 0 to 2. Moreover,

$$\left(d_j^\dagger\right)^2 = 2\left(d_i^1\right)^\dagger \left(d_i^2\right)^\dagger, \tag{B7}$$

that means $\left(d_j^\dagger\right)^3 = 0$. Therefore, the parafermion representation provides the extended Pauli exclusion principle.

To establish a connection between the bond g-algebra and the parafermion statistics, we note that the local Hilbert space related with a bond has the dimension $D = 3$. Therefore, one can map the g-particles onto the algebra of S-1 operators

$$S_i^+ = \sqrt{2} g_i^\dagger \left[1 + \left(\frac{1}{\sqrt{2}} - 1\right) n_i^g\right],$$

$$S_i^- = \sqrt{2}\left[1 + \left(\frac{1}{\sqrt{2}} - 1\right) n_i^g\right] g_i, \tag{B8}$$

$$S_i^z = n_i^g - 1.$$

These spin operators are connected with two-flavour hard-core bosons via the generalization of the Jordan-Wigner transformation[23,24]

$$\begin{gathered} S_i^+ = \sqrt{2}\left(b_{i1}^\dagger + b_{i2}\right), \\ S_i^- = \sqrt{2}\left(b_{i1} + b_{i2}^\dagger\right), \\ S_i^z = b_{i1}^\dagger b_{i1} - b_{i2}^\dagger b_{i2} \end{gathered} \tag{B9}$$

with the imposed constraint $b_{i1}^\dagger b_{i1} + b_{i2}^\dagger b_{i2} = 1$, and the spin state $S^z = 0$ is taken as a vacuum. The commutation relations for the hard bosons are

$$[b_{i\alpha}, b_{i\beta}] = \left[b_{i\alpha}^\dagger, b_{i\beta}^\dagger\right] = 0,$$

$$\left[b_{i\alpha}, b_{i\beta}^\dagger\right] = \delta_{ij}\delta_{\alpha\beta}\left(1 - n_{i\alpha}^b\right), \quad \left[n_{i\alpha}^b, b_{j\beta}^\dagger\right] = \delta_{ij}\delta_{\alpha\beta} b_{i\alpha}^\dagger, \tag{B10}$$

where $n_{i\alpha}^b = b_{i\alpha}^\dagger b_{i\alpha}$ $(\alpha = 1, 2)$ is the number operator for the hard bosons.

A transition from the hard-core bosons to the parafermions is related with a transmutation of statistics. In two-dimensional case the change of statistics is based on a generalization of the conventional Jordan-Wigner transformation.[25,26] In the following, for simplicity, we illustrate the connection on an example of dimerized one-dimensional S-1 chain.

The parafermion modes are converted into the canonical two-flavour canonical fermions $c_{i\alpha}$ $(\alpha = 1, 2)$ determined on the i-th bond of the chain through the *partial* non-local transmutators

$$\left(d_i^1\right)^\dagger = c_{i1}^\dagger \exp\left[i\pi \sum_{j<i} n_{j2}\right], \quad \left(d_i^2\right)^\dagger = c_{i2}^\dagger \exp\left[i\pi\left(\sum_{j<i} n_{j1} + n_{i1}\right)\right], \tag{B11}$$

where

$$\{c_{i\alpha}, c_{j\beta}\} = \left\{c_{i\alpha}^\dagger, c_{j\beta}^\dagger\right\} = 0, \quad \left\{c_{i\alpha}, c_{j\beta}^\dagger\right\} = \delta_{ij}\delta_{\alpha\beta}, \tag{B12}$$

and $n_{i\alpha} = c^\dagger_{i\alpha} c_{i\alpha}$ is the number operator for the fermions.

A map between the hard-core bosons and the two-flavour fermions is established by the *total* non-local transmutators

$$b^\dagger_{i1} = c^\dagger_{i1} \exp\left[i\pi \sum_{j<i} \left(c^\dagger_{j1} c_{j1} + c^\dagger_{j2} c_{j2} \right) \right],$$

$$b^\dagger_{i2} = c^\dagger_{i2} \exp\left[i\pi \sum_{j<i} \left(c^\dagger_{j1} c_{j1} + c^\dagger_{j2} c_{j2} \right) \right] e^{i\pi c^\dagger_{j_1} c_{j_1}}. \tag{B13}$$

The relations (B8,B9,B11,B13) provide a map between the parafermions and the g-particles.

[1] I. Affleck, Phys. Rev. B **41**, 6697 (1990); T. Giamarchi and A.M. Tsvelik, Phys. Rev. B **59**, 11398 (1999).
[2] T. Giamarchi, C. Rüegg, O. Tchernyshyov, Nature Phys. **4**, 198 (2008).
[3] T. M. Rice, Science **298**, 760 (2002).
[4] T. Nikuni etal., Phys. Rev. Lett. **84**, 5868 (2008).
[5] C. Rüegg et al., Nature (London) **423**, 62 (2003).
[6] S.E. Sebastian et al., Nature (London) **441**, 617 (2006).
[7] M.Kofu, J.-H. Kim, S. Ji, S.-H. Lu, H.Ueda, Y. Qin, H.-J. Kang, M.A. Green, and Y. Ueda, Phys. Rev. Lett. **102**, 037206 (2009).
[8] H. Tsuji, B. Andraka, M. Ushida, H. Tanaka, Y. Takano, Phys. Rev. B **72**, 214434 (2005).
[9] M.B. Stone, M.D. Lumsden, S. Chang, E.C. Samulon, C.D. Batista, I.R. Fisher, Phys. Rev. Lett. **100**, 237201 (2008).
[10] C.D. Batista, G. Ortiz, Adv. in Physics **53**, 1 (2004).
[11] P. Sengupta and C.D. Batista, Phys. Rev. Lett. **98**, 227201 (2007).
[12] Y. Hosokoshi, Y. Nakazawa, K. Inoue, K. Takizawa, H. Nakano, M. Takahashi, T. Goto, Phys. Rev. B **60**, 12924 (1999).
[13] H. Tsujii, B. Andraka, Y. Hosokoshi, K. Inoue, and Y. Takano, JMMM **310**, 415 (2007).
[14] A.S. Boyarchenkov, I.G. Bostrem, A.S. Ovchinnikov, Phys. Rev. B **76**, 123456 (2007).
[15] V.E. Sinitsyn, I.G. Bostrem,A.S. Ovchinnikov, J. Phys. A: Math. Theor. **40**, 645 (2007).
[16] M. Sato, Phys. Rev. B **71**, 024402 (2005).
[17] T. Sakai and M. Takahashi, Phys. Rev. B **43**, 13383 (1991); ibid. **57**, R3201 (1998).
[18] M. Grenier, O. Mandel, T. Esslinger, T.W. Hänsch, I. Bloch, Nature **415**, 39 (2002).
[19] I. Bloch, Nature Phys. **1**, 23 (2005).
[20] F.D.M. Haldane, Phys. Rev. Lett. **67**, 937 (1991).
[21] H.S. Green, Phys. Rev. **90**, 270 (1953).
[22] H.S. Green, Prog. Theor. Phys. **47**, 1400 (1972).
[23] C.D. Batista, G. Ortiz, Phys. Rev. Lett. **86**, 1082 (2001).
[24] P. Sengupta, C.D. Batista, Phys. Rev. Lett. **99**, 2172205 (2007).
[25] E. Fradkin, Phys. Rev. Lett. **63**, 322 (1989).
[26] Y.R. Wang, Phys. Rev. B **43**, 3786 (1991).